Application of L0-Norm Regularization to Epicardial Potential Reconstruction

Liansheng Wang[1], Xinyue Li[1], Yiping Chen[1], and Jing Qin[2,3]

[1] Department of Computer Science, School of Information Science and Engineering, Xiamen University, Xiamen, China
lswang@cse.cuhk.edu.hk
[2] School of Medicine, Shenzhen University, China
[3] Guangdong Key Laboratory for Biomedical Measurements and Ultrasound Imaging, China

Abstract. Inverse problem of electrocardiography (ECG) has been extensively investigated as the estimated epicardial potentials (EPs) reflecting underlying myocardial activities. Traditionally, L2-norm regularization methods have been proposed to solve this ill-posed problem. But L2-norm penalty function inherently leads to considerable smoothing of the solution, which reduces the accuracy of distinguishing abnormalities and locating diseased regions. Directly using L1-norm penalty function, however, may greatly increase the computational complexity due to its non-differentiability. In this study, we present a smoothed L0 norm technique in order to directly solve the L0 norm constrained problem. Our method employs a smoothing function to make the L0 norm continuous. Extensive experiments on various datasets, including normal human data, isolated canine data, and WPW syndrome data, were conducted to validate our method. Epicardial potentials mapped during pacing were also reconstructed and visualized on the heart surface. Experimental results show that the proposed method reconstructs more accurate epicardial potentials compared with L1 norm and L2 norm based methods, demonstrating that smoothed L0 norm is a promising method for the noninvasive estimation of epicardial potentials.

1 Introduction

Inverse ECG problem has been paid much attention recently as it is an efficient tool for the characterization of cardiac electrical events. In the study of ECG inverse problem, the electrical activity of the heart can be described by the reconstructed epicardial potentials [1]. In our study, supposing the torso surface potentials are given, we attempt to compute the potentials on the epicardial surface.

As it subjects to both the Dirichlet and Neumann boundary conditions, this problem is a boundary value problem. Assuming the human torso is homogeneous and isotropic, this boundary value problem can be solved by a boundary element method (BEM), which relates the potentials at the torso nodes (expressed as a m-dimensional vector Φ_T) to the potentials at the epicardial nodes (expressed as a n-dimensional vector Φ_E):

$$\Phi_T = A\Phi_E \tag{1}$$

where A is the transfer coefficient matrix $(m * n)$ with $n < m$. The transfer coefficient matrix A is determined entirely by the geometric integrands and thus can be calculated analytically with a BEM solution.

N. Navab et al. (Eds.): MICCAI 2015, Part II, LNCS 9350, pp. 493–500, 2015.
DOI: 10.1007/978-3-319-24571-3_59

To find a practical solution, regularization is usually employed to tackle the ill-posedness and reduce the outliers of the inverse solution [2]. In these regularizations, Tikhonov regularizations with zeroth, first, and second orders impose constraints on the magnitude or derivatives of the epicardial potential Φ_E to overcome the ill-posed inverse problem [3] [4]. The truncated total least squares (TTLS) method is introduced to solve the inverse problem with adaptive BEM in [5]. TTLS can deal with the measurement errors and geometry errors at the same time, but it suffers from large reconstruction errors when the measurement errors and geometry errors increase. These regularizations are all in the L2 norm which will smooth the reconstructed results.

Except L2 norm regularization, total variation (TV) has been recently applied to the inverse problem of ECG and achieve good comparable results in terms of L_1-norm [6] [7]. However, the implementation of TV is complicated due to the non-differentiability of the penalty function with L_1-norm.

L0 norm is an efficient scheme for solving the inverse problem of ECG. However, due to the discontinuity of the penalty function, investigators had to develop L2 norm methods and L1 norm methods to approximate the L0 norm [8]. In this study, we present a smoothed L0 norm solution [9] to epicardial potential reconstruction which directly solves the inverse problem of ECG. Through a smooth measure approximating the L0 norm, a smoothed L0 norm solves the inverse problem in an iterative manner. The smoothed L0 norm is validated on various datasets, including isolated canine heart data, normal human data, and WPW syndrome data.

2 The Smoothed L0-Norm Method

The inverse problem of ECG can be carried out by solving the unconstrained minimization:

$$min\{\|A\Phi_E - \Phi_T\|_2 + \lambda \|\Phi_E\|_0\} \tag{2}$$

where λ is the regularization parameter. However, as discussed, the L0 norm faces two challenges. The first is the discontinuity which means that we have to perform a combinatorial search for its minimization. The second is its high noise sensitivity. We meet these two challenges by employing a smoothed L0-norm method.

The main idea of the smoothed L0 is to employ a smoothing function (continuously) for the L0 norm minimization. For the inverse problem of ECG, we approximate the L0 norm of the potential vector Φ_E by a smoothing function $F_\sigma(\Phi_E)$, where the value of σ controls the accuracy of the approximation.

Given the potential vector $\Phi_E = [\phi_1, ..., \phi_n]^T$, the L0 norm of Φ_E is valued as the number of the non-zero components in Φ_E. We define it as follows:

$$\nu(\phi) = \begin{cases} 1 & \phi \neq 0 \\ 0 & \phi = 0. \end{cases} \tag{3}$$

Thus, the L0 norm of Φ_E can be expressed as:

$$||\Phi_E||_0 = \sum_{i=1}^{n} \nu(\phi_i). \tag{4}$$

It is obvious that the L0 norm is discontinuous because of the discontinuities of the function v. If we can replace v with a continuous function, the L0 norm will be continuous. With the smoothed L0 norm, we apply the zero-mean Gaussian family of functions for the inverse problem of ECG. By defining:

$$f_\sigma(\phi) = \exp(-\phi^2/2\sigma^2), \tag{5}$$

we have:

$$\lim_{\sigma\to 0} f_\sigma(\phi) = \begin{cases} 1 & \phi = 0 \\ 0 & \phi \neq 0, \end{cases} \tag{6}$$

and thus we can obtain:

$$\lim_{\sigma\to 0} f_\sigma(\phi) = 1 - v(\phi). \tag{7}$$

Then, we define:

$$F_\sigma(\phi) = \sum_{i=1}^{n} f_\sigma(\phi_i), \tag{8}$$

and the L0 norm of Φ_E is approximated with $n - F_\sigma(\phi)$:

$$||\Phi_E||_0 = n - F_\sigma(\phi). \tag{9}$$

The σ determines the effect of the approximation. If the σ is too large, the approximation will be too smooth to accurately reflect the L0 norm of Φ_E. If the σ is too small, it is easily trapped in the local minima searching for σ. We employ the scheme proposed in the Graduated Non-Convexity (GNC) [10] method to control the value of σ for escaping from the local minima, where the value of σ is decreased gradually.

The final smoothed L0 norm for the inverse problem of ECG is summarized in the following algorithm:

Algorithm 1. Smoothed L0 norm method for inverse problem of ECG

1: **(Initialization)**:
   1. Given $\widehat{\phi}$ as an arbitrary solution to the inverse problem of ECG obtained from a pseudo-inverse of A.
   2. Choose a suitable decreasing sequence for σ, $[\sigma_1, ..., \sigma_K]$.
2: **(FOR Loop)**:k=1,...,K
   1. Let $\sigma = \sigma_j$;
   2. Maximize (approximately) the function F_σ on the feasible set of inverse problems of ECG using L iterations of the steepest ascent algorithm
   (1)Initialization: $\phi = \widehat{\phi}_j$.
   (2)for $j = 1, ..., L$ (loop L times):
   (a)$\delta \stackrel{\Delta}{=} [\phi_1 \exp(-\phi_1^2/2\sigma^2), ..., \phi_n \exp(-\phi_n^2/2\sigma^2)]^T$
   (b) Let $\phi \leftarrow \phi - \omega\delta$ (where ω is a small positive constant).
   (c) Project ϕ back onto the feasible set: $\phi \leftarrow \phi - A^T(AA^T)^{-1} - (A\phi - \Phi_T)$.
   3. Set $\widehat{\phi}_j = \phi$.
3: **(END FOR Loop)**
4: **(Results)**: $\widehat{\phi} = \widehat{\phi}_K$.

3 Experimental Data and Protocols

In order to evaluate the proposed smoothed L0 norm, L2 norm method TTLS (L2-TTLS) [5] and L1 norm method GPSR (L1-GPSR) [8] are compared with our presented method. In the experiments, the slowly decreasing sequences of σ are fixed to $[1, 0.5, 0.2, 0.1, 0.05, 0.02, 0.01]$ and δ is fixed to 2.5 based on our data.

3.1 Data

Three different types of data were used in our experiments.

Normal Human Data. Three normal male data were collected for the normal case study. The geometric heart model and torso model were built from MRI scanning images. The high-resolution 65-lead body surface potential mapping were collected for these normal cases.

Isolated Canine Heart Data. The normal canine data is obtained from the Center for Integrative Biomedical Computing (CIBC) at the University of Utah. The details of the data collection procedure are reported in [11]. The torso surface potentials are computed in a forward solution. A homogenous torso geometry including the epicardial sock electrodes (490 nodes and 976 triangles) and torso tank (771 nodes and 1254 triangles) is used in the forward solution. The forward solution used BEM from Matti Stenroos *et al.* [12]. To mimic the realistic conditions, $25dB$ signal-to-noise (SNR) Gaussian noise (independent, zero mean) are added to the computed torso surface potentials. The added noise is zero mean and unit standard variation distribution.

WPW Syndrome Data. The WPW syndrome data was collected from seven patients (3 female) with overt ventricular pre-excitation who underwent an electrophysiologic examination. The patients were as assessed through prior transthoracic echocardiography to make sure they had structurally normal hearts for this study. Patients in this study had not received antiarrhythmic drug therapy [13].

3.2 Evaluation Protocols

We quantitatively evaluate the accuracy of the ECG inverse problem by using two standard criteria: relative error (RE) and correlation coefficient (CC). The RE is defined as:

$$RE = \frac{||\Phi_H - \hat{\Phi}_H||_2}{||\hat{\Phi}_H||_2}, \tag{10}$$

and the CC is defined as:

$$CC = \frac{\sum_{k=1}^{N_k} (\Phi_H(k) - \bar{\Phi}_H(k))(\hat{\Phi}_H(k) - \bar{\hat{\Phi}}_H(k))}{\sqrt{\sum_{k=1}^{N_k} (\Phi_H(k) - \bar{\Phi}_H(k))^2 \sum_{k=1}^{N_k} (\hat{\Phi}_H(k) - \bar{\hat{\Phi}}_H(k))^2}}, \tag{11}$$

where N_k is the total number of nodes on the heart geometry surface. The Φ_H is the potential value on the heart surface. The superscript '$\hat{}$' refers to the reference values and the superscript '$\bar{}$' refers to the mean values.

4 Experiments and Results

In our experiments, all methods were implemented in MATLAB R2012a running on a Dell computer with Intel Core2 i3-2120 CPU 3.30GHz and 4.00GB RAM.

Figure 1 shows the epicardial potential maps of human data during pacing, 13ms after onset of QRS. Measured data is shown in figure 1(a) with the pacing site marked by an plus sign. Elliptic shapes of negative potential (in dark blue) spread out as a round shape into two sides of positive potentials areas (in red). Figure 1(b) shows reconstructed data by L2-TTLS. While L2-TTLS reconstructs the pattern of negative potentials (in dark blue) around the pacing site (plus sign) flanked by a broad area of positive potentials (in red), it overestimates the spatial gradients between the area of negative potentials and the area of positive potentials on the sides, which leads to significant errors in the reconstructions with high RE (RE=0.36) and low CC (CC=0.65). Figure 1(c) shows the reconstructed results by the L1-GPSR [8]. Although the reconstruction accuracy improves (RE=0.19, CC=0.88), the negative potentials around the pacing site are also overestimated, which is shown in a big parallel circle. The L0-norm solution ((RE=0.10, CC=0.97)) demonstrates high fidelity compared with the measured data shown in figure 1(d), in which the shape of the negative potentials is well preserved. More importantly, the spatial gradients (blue to red) around the pacing site are more accurately estimated. The values of the RE and CC also show the highest reconstruction accuracy and best spatial features compared to the L2-norm and L1-norm methods.

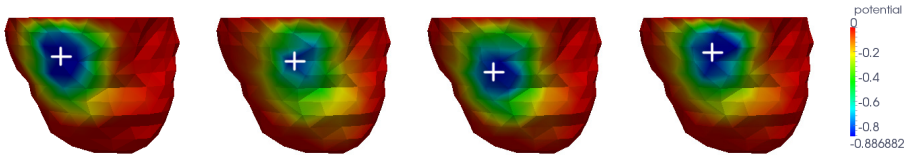

(a) Measured (b) L2-TTLS (c) L1-GPSR (d) L0 Norm (e)

Fig. 1. Reconstructed epicardial potential maps, 13ms after onset of QRS, for different methods. The plus sign shows the pacing site. The unit of potential is V.

Figure 2 shows the epicardial electrograms of the pre- and post-infarction. Two epicardial sites are chosen; marked on the surface of the heart. Site 1 is chosen within the infarct area and site 2 is chosen away from the infarct area. While the form of the electrograms at site 2 remains unchanged in the pre-infarct and post-infarct, electrograms at site 1 are reversed in negative and positive. The L0-norm solution preserves better form of the electrograms compared to L2-TTLS and L1-GPSR in terms of RE and CC.

QRST integral mapping has been shown to be a useful noninvasive method to assess the spatial distribution of primary ventricular recovery properties [14]. QRST integral maps were computed by using of the sum of all potentials from the QRS onset to the T-wave offset in each lead. The epicardial QRST integral maps of the canine data computed from measured and reconstructed data are shown in figure 3. The warm area of the LV with high QRST integral values is shown in red color while the cooler region

with lower values is shown in dark blue. Although the reconstructed maps achieve the low and high QRST integral values, the L2-TTLS solution shows over-computed high integral values with larger RE (RE=0.78). Meanwhile, parts of the high integral values are missed in the result of the L1-GPSR solution with a lower CC (CC=0.57). Our L0-norm method achieved the best results.

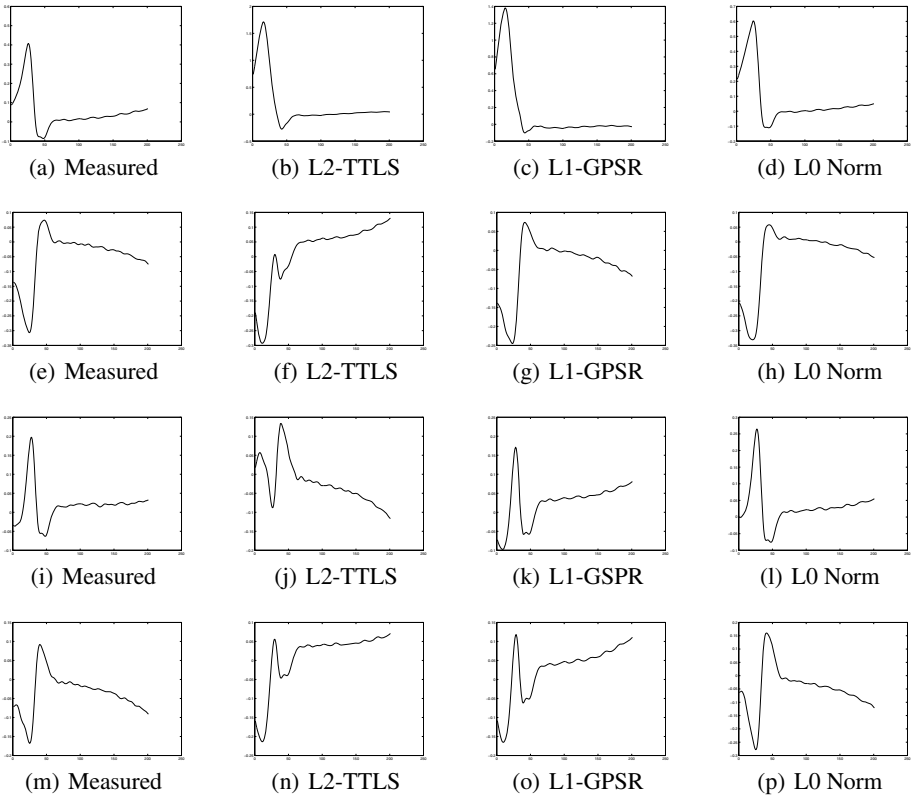

Fig. 2. Measured and reconstructed electrograms by L2-norm, L1-norm and L0-norm methods. The upper two rows are for site 1 and bottom two rows are for site2. For site 1 and site 2, the first row for pre-infarct and the second row for post-infarct.

Figure 4 shows the epicardial activation map in a male patient with WPW syndrome. The time step for this activation isochrones is 2ms. The L2-norm solution shows a large flat area of early activation (in pink color) while the L1-norm solution shows the one distinct early activation areas which means there is one diseased region. However, the L0-norm solution shows two distinct early activation areas of which one early activation area cannot be found in the L1-norm solution. These two distinct areas of early activation are very important for surgeons making a surgical plan. The reconstructed results demonstrate that the proposed L0-norm method achieves more accurate results than the L2-TTLS method and the L1-GPSR method.

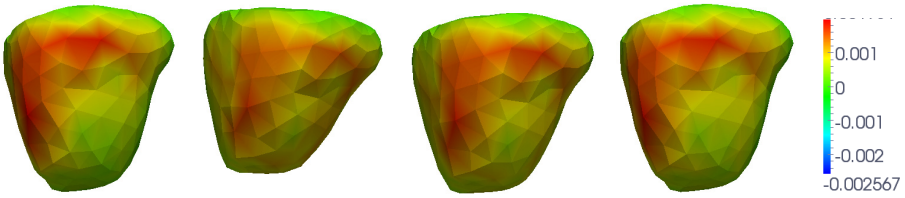

(a) Measured (b) L2-TTLS (c) L1-GPSR (d) L0 Norm (e)

Fig. 3. Epicardial QRST integral maps from measured and reconstructed data. The unit is $V - ms$.

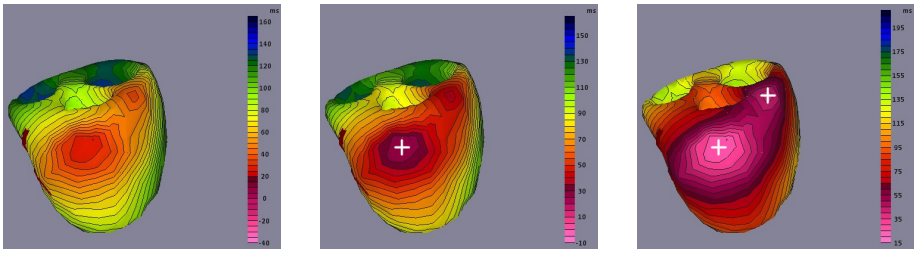

(a) L2-TTLS (b) L1-GPSR (c) L0 Norm

Fig. 4. Activation maps for Wolff Parkinson White (WPW) patient reconstructed by the L2 norm, L1 norm, and L0 norm. The plus sign indicates the distinct early activation area.

5 Conclusion

A L0-norm base regularization technique was applied to the inverse problem of ECG for epicardial potentials reconstruction in this study. In order to overcome the discontinuity of the L0 norm, a smooth measure is employed for direct reconstruction of epicardial potentials in an iterative manner. The experiments were conducted in different types data of isolated canine heart, normal human, and patients with WPW syndrome. The reconstructed results were compared to the L2-norm based method and the L1-norm based method. Experimental results showed that the proposed L0-norm base method is a promising method for the inverse problem of ECG which achieves more accurate results than L2-norm and L1-norm based methods.

Acknowledgement. This work was supported by National Natural Science Foundation of China (Grant No. 61301010), the Natural Science Foundation of Fujian Province (Grant No. 2014J05080), Research Fund for the Doctoral Program of Higher Education (20130121120045), by CCF-Tencent Open Research Fund and by the Fundamental Research Funds for the Central Universities (Grant No. 2013SH005, Grant No. 20720150110).

References

1. Wang, D., Kirby, R.M., Johnson, C.R.: Resolution Strategies for the Finite-Element-Based Solution of the ECG Inverse Problem. IEEE Transactions on Biomedical Engineering 57(2), 220–237 (2010)
2. Milanic, M., Jazbinsek, V., Wang, D., Sinstra, J., MacLeod, R.S., Brooks, D.H., Hren, R.: Evaluation of approaches to solving electrocardiographic imaging problem. In: IEEE Computers in Cardiology, pp. 177–180 (2010)
3. Dössel, O.: Inverse problem of electro-and magnetocardiography: Review and recent progress. International Journal of Bioelectromagnetism 2(2) (2000)
4. Rudy, Y., Messinger-Rapport, B.J.: The inverse problem in electrocardiography: Solutions in terms of epicardial potentials. Critical Reviews in Biomedical Engineering 16(3), 215–268 (1988)
5. Shou, G., Xia, L., Jiang, M., Wei, Q., Liu, F., Crozier, S.: Truncated total least squares: a new regularization method for the solution of ECG inverse problems. IEEE Transactions on Biomedical Engineering 55(4), 1327–1335 (2008)
6. Ghosh, S., Rudy, Y.: Application of L1-norm regularization to epicardial potential solution of the inverse electrocardiography problem. Annals of Biomedical Engineering 37(5), 902–912 (2009)
7. Shou, G., Xia, L., Liu, F., Jiang, M., Crozier, S.: On epicardial potential reconstruction using regularization schemes with the L1-norm data term. Physics in Medicine and Biology 56, 57–72 (2011)
8. Wang, L., Qin, J., Wong, T., Heng, P.: Application of l1-norm regularization to epicardial potential reconstruction based on gradient projection. Physics in Medicine and Biology 56, 6291 (2011)
9. Mohimani, H., Babaie-Zadeh, M., Jutten, C.: A fast approach for overcomplete sparse decomposition based on smoothed norm. IEEE Transactions on Signal Processing 57(1), 289–301 (2009)
10. Blake, A., Zisserman, A.: Visual reconstruction. MIT Press, Cambridge (1987)
11. MacLeod, R.S., Lux, R.L., Taccardi, B.: A possible mechanism for electrocardiographically silent changes in cardiac repolarization. Journal of Electrocardiology 30, 114–121 (1998)
12. Stenroos, M., Haueisen, J.: Boundary element computations in the forward and inverse problems of electrocardiography: comparison of collocation and Galerkin weightings. IEEE Transactions on Biomedical Engineering 55(9), 2124–2133 (2008)
13. Berger, T., Fischer, G., Pfeifer, B., Modre, R., Hanser, F., Trieb, T., Roithinger, F., Stuehlinger, M., Pachinger, O., Tilg, B., et al.: Single-beat noninvasive imaging of cardiac electrophysiology of ventricular pre-excitation. Journal of the American College of Cardiology 48(10), 2045–2052 (2006)
14. Wilson, F., Macleod, A., Barker, P., Johnston, F.: The determination and the significance of the areas of the ventricular deflections of the electrocardiogram. American Heart Journal 10(1), 46–61 (1934)